Robert L. Mairs*
*NOAA National Environmental Satellite Service*
*Hillcrest Heights, Md. 20031*
Dennis K. Clark†
*U.S. Naval Oceanographic Office*
*Washington, D.C. 20390*

# Remote Sensing of Estuarine Circulation Dynamics

**Repetitive remotely sensed data coupled with a well equipped concurrent surface data collection program can provide extremely useful information on the complexity of estuarine flow.**

Abstract: *Multispectral and color aerial photography and infrared imagery of naturally occurring water color boundaries and/or dye tracer implants have been used successfully in the study of temporal coastal and estuarine circulation dynamics. Sequential photography and high-contrast enhancements of color imagery of fronts such as foam lines, current shears, etc., along with point and line sources of fluorescein dye are used to calculate and plot displacements and velocity vectors of water masses along the North Carolina coast and in the Patuxent River estuary, Maryland. Techniques have been developed for incorporation of remotely sensed data which are collected on a temporal scale ranging from minutes to hours, with extensive surface truth measurements to describe further the complex nature of estuarine flow.*

## Introduction

The understanding and management of our coastal environment and the impact made upon it by estuarine effluents is rapidly becoming a major problem for United States regulatory agencies. Expanded utilization of this valuable natural resource results in increased demands upon these agencies for decisions for which there is little or no background material.

Although 71 percent of the earth's surface is covered by ocean water, only 6 percent lies within the boundaries of the continental shelves, yet this portion of the ocean has historically been most significant to mankind. The knowledge of circulation dynamics within these boundaries along the Mid-Atlantic coasts of the United States and the resulting dispersal of suspended and dissolved substances which are naturally and culturally introduced from the continent is very fragmentary. The dilution capacities of many of our nation's coastal waterways are becoming increasingly taxed because of the expansion of population and industry bordering our coastlines.

This lack of knowledge concerning estuarine circulation dynamics is proving costly and threatens the natural utility of these waterways. With the rapid development of remote-sensor technology, a new technique for ocean monitoring is evolving. Remote sensors are now capable of providing an overview of surface and near-surface conditions in real time over large geographical areas, and are particularly amenable to estuarine circulation research.

The objectives of this nearshore remote-sensing research, which hopefully will lead to a better understanding of the above mentioned problems, are: (1) attempt to describe surface and near-surface fluid flow dynamics in an estuarine environment using synoptic aerial photography and infrared imagery, (2) attempt to establish the temporal characteristics of various surface and near-surface coastal features, and (3) correlate the spatial and temporal characteristics of

* Now with Earth Satellite Corporation, Washington, D.C. 20006.
† Now with NOAA National Environmental Satellite Service, Hillcrest Heights, Md. 20031.

estuarine effluents with other environmental parameters.

## Rationale

Two major study components are to be considered in any remote-sensing experiment: surface and remote data collection. Surface, or ocean truth, data are essential to remote-sensing research if specific properties of the environment are to be uniquely related to the characteristics of the remotely sensed image. Surface and subsurface measurements taken simultaneously with the remotely sensed data are particularly important where the environment is undergoing constant change as in coastal waters.

In studying the ocean's surface with electromagnetic sensors, two fundamental properties require understanding. The first property is the dynamic nature of the ocean's surface; how it can change from a mirror smooth surface acting as a specular scatterer under no wind-wave conditions to white water under heavy winds. The second property is the degree to which electromagnetic energy can penetrate the water itself. Significant water penetration occurs only in two general regions of the spectrum; at very long wavelengths around 100 to 200 kilometers and at shorter wavelengths around 400 to 600 nanometers (nm). As it is impractical to build remote sensors at long wavelengths because of the power problem, the only portion available for penetration of water lies in the visible region from about 400 to 600 nm (Sherman, 1971).

The main energy source for image information on photographic film is the sun. The amount of solar energy which is recorded by photographic film in any particular wavelength band depends upon the energy which: (1) strikes the water's surface, (2) reaches a subsurface object, (3) is reflected by the object, and (4) makes its way coherently back through the water and across the water-air interface (Yost, et al, 1971). Much of the

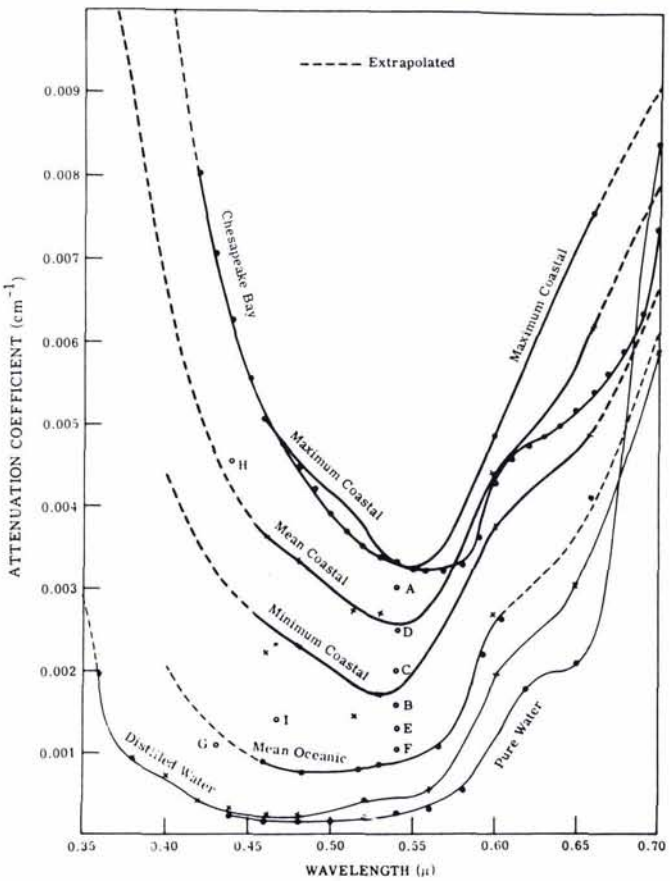


Fig. 1. Attenuation coefficient versus wavelength for pure water and various types of ocean water (from Polcyn and Rollin, 1969).

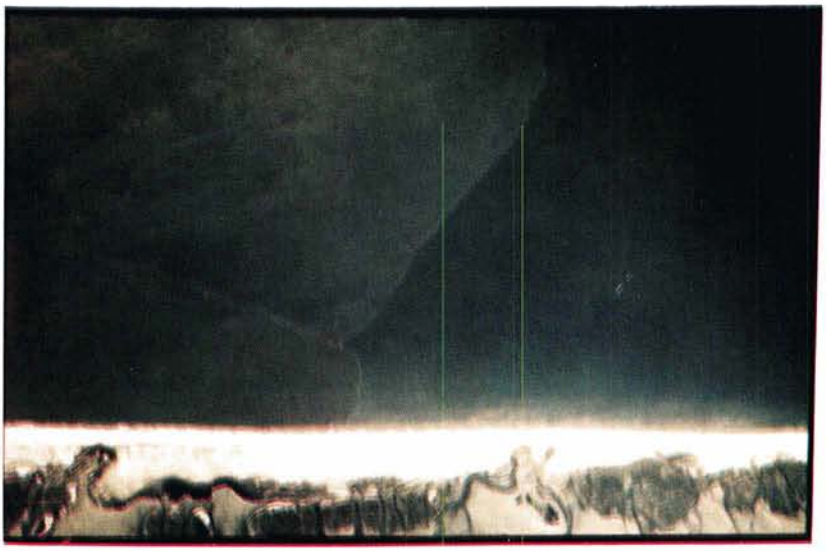

**Plate 1.** Color photograph of an estuarine plume front adjacent to the North Carolina coast (17 November 1970).

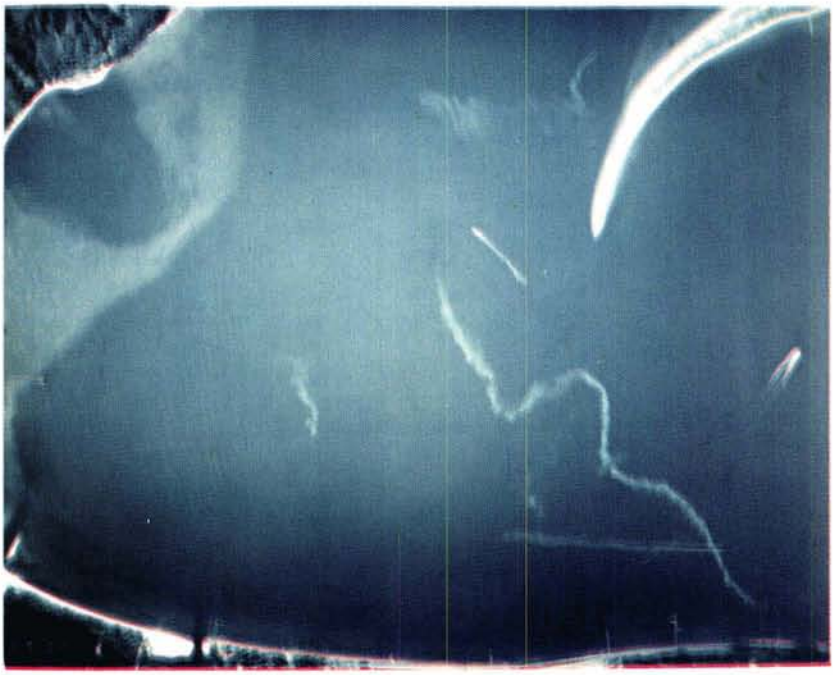

**Plate 2.** Point and line dye sources, Point Patience vicinity, 14 May 1971 (1642 EDT).

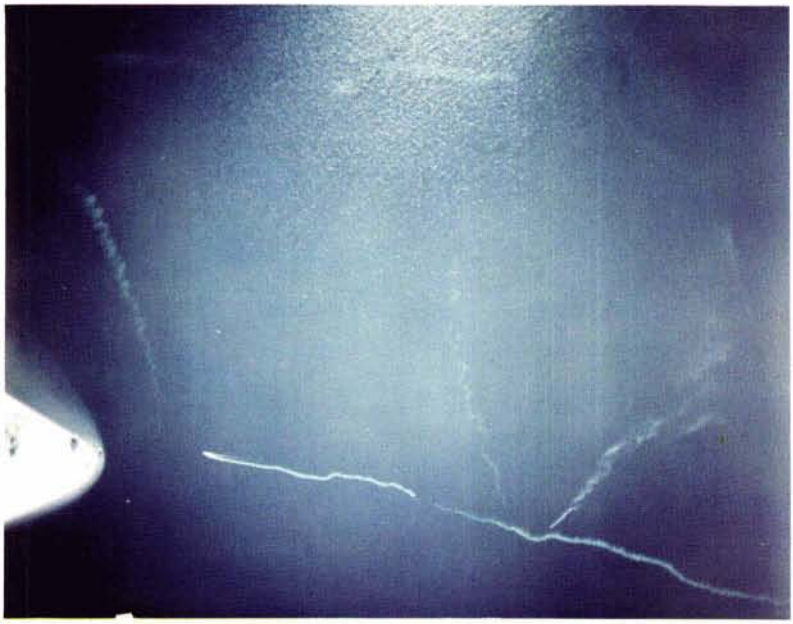

**Plate 3.** Point and line dye sources between Drum and Fishing Points, 14 May 1971 (0842 EDT). (North is toward the left).

**Plate 4.** Point and line dye sources between Drum and Fishing Points, 14 May 1971 (0848 EDT). (North is toward the left)

image information energy that reaches the camera from below the water's surface is concentrated in a spectral region extending from about 420 to 550 nm.

In relatively clear oceanic waters, peak transmission occurs near 480 nm. As one moves into coastal waters which contain a complex mixture of solubles, colloids, suspensoids, and biological matter, visible light is absorbed, scattered and reflected in different spectral bands and in varying amounts, which effectively shifts the transmission peak towards the green. The attenuation coefficients for several types of water from wavelengths of 350 to 700 nm and the shift in peak transmission from the blue to the green as the water-type changes from open ocean to that of coastal regions can clearly be seen in Figure 1. Figure 1 also shows how the attenuation coefficient increases as one moves from the blue to the red end of the spectrum. By studying data such as these, varying portions of the visible spectrum can be chosen depending on the study application and the type of water to be looked at. As an example, in clear ocean water, increased depth penetration is found with transition from the red to the green to the blue.

By choosing spectral filters corresponding to these particular wavelengths, a three-dimensional rendition of the ocean environment can be obtained. The response of light energy can be illustrated on a qualitative basis by using the NASA MSC six-band Hasselblad camera array which records on film several discrete portions of the visible spectrum (Figure 2). These filter combinations were chosen by the authors to record the light energy that corresponds best to that upwelled from turbid coastal waters.

Remote-sensor technology is particularly applicable to nearshore circulation studies because of naturally occurring color fronts, tide lines, foam lines, current shears, etc., which frequently are found along coastlines, harbors, and estuaries. These boundaries, separating water masses, are observed in and near every estuary along our East coast where river or estuarine water flushes periodically into the ocean as a result of tidal action.

Where these naturally occurring color fronts do not exist or where more detailed knowledge of the circulation dynamics are needed, dye tracer techniques may be utilized to study the complex fluid flow in the estuarine system.

## Methods of Approach

In November 1970, the North Carolina coast between Capes Hatteras and Lookout was the site of a NASA MSC Earth Resources remote-sensing mission utilizing the high altitude (60,000 feet) RB57F aircraft. The flight objective was to obtain high-altitude overlapping multispectral photography over the coastal waters at least twice during a tidal cycle. Extensive ocean truth measurements of suspended particulates, temperature, salinity, depth, Secchi depth, climatological, and surface and subsurface spectroradiometric data were taken concurrently with the overflights.

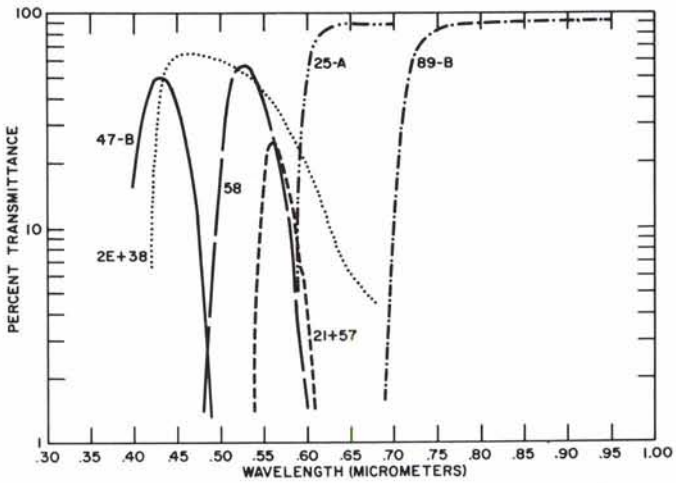


Fig. 2. Multispectral filter transmission characteristics of the Hasselblad camera array.

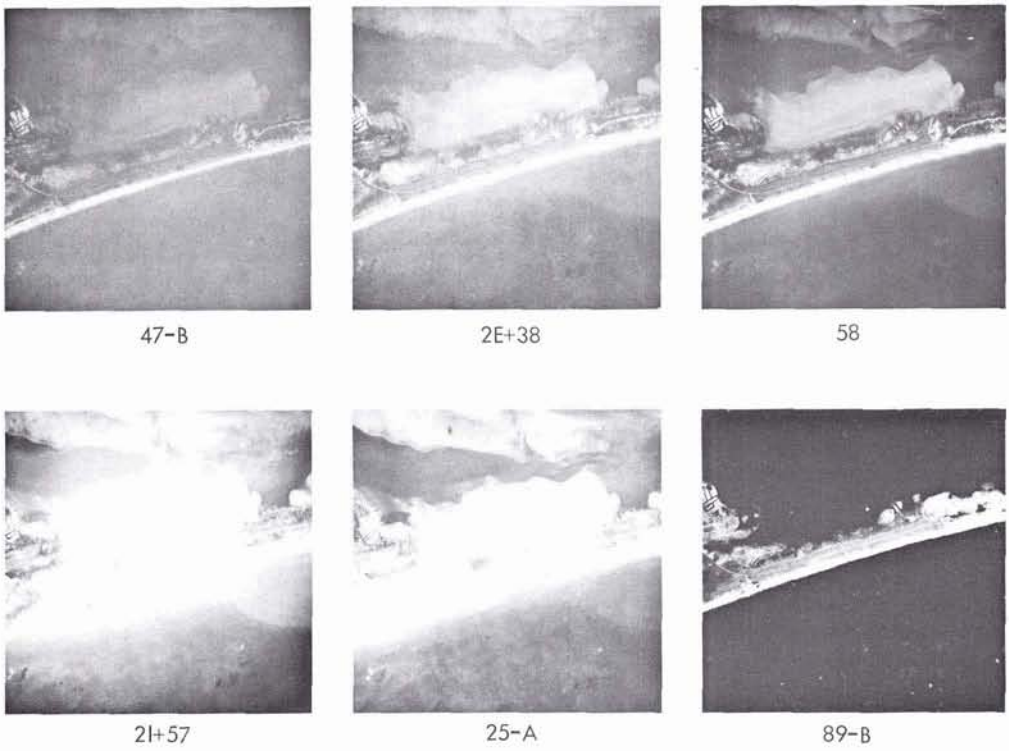


FIG. 3. Six simultaneous multispectral photographs of an estuarine plume front along the North Carolina coast, 17 November 1970.

The six simultaneous multispectral photographs (Figure 3) of an estuarine plume front adjacent to the North Carolina coast illustrate a qualitative comparison of the six filter combinations chosen for water mass delineation. Starting at the blue end (47-B) of the spectrum, very little contrast or definition can be seen in the water due to increased attenuation of the signal both by the contaminated atmosphere found over most terrestrial regions and also by the suspended and dissolved substances in the water.

As one moves to the blue-green (2E+38), the green (58), the yellow (21+57), and the red (25−A), increasing contrast and definition of the plume front can be observed. The near infrared energy (89−B) is completely absorbed at the surface and gives no information on subsurface phenomena, but shows excellent shoreline definition. The portion of the visible spectrum from the upper green through the orange seems to give the best depth penetration, contrast, and definition for these particular waters. Spectroradiometric data taken shortly after the flights confirmed the observation that in highly turbid waters the deepest penetration was by that portion of the visible spectrum from about 550 to 610 nm.

The color photograph (Plate 1) of an estuarine plume front, taken during the same NASA mission, illustrates the limited tonal and density differences found from one side of the plume front to the other and the difficulty of detailed delineation of that front. This plume front or tide line is manifest at the surface and is observed to be a long, continuous, meandering line of foam, detritus, and trash. This accumulation of matter suggests a zone of convergence and indicates the line of intersection between two water masses.

A number of optical and photographic enhancement techniques were utilized in an attempt to increase the delineation of this plume front. No advantages could be found by using the optical enhancers; however, photographic techniques provided satisfactory contrast level information. A high-contrast enhancement (Figure 4) clearly illustrates the increased definition of the plume front and the three separate water masses along the coastline. Suspended particulate

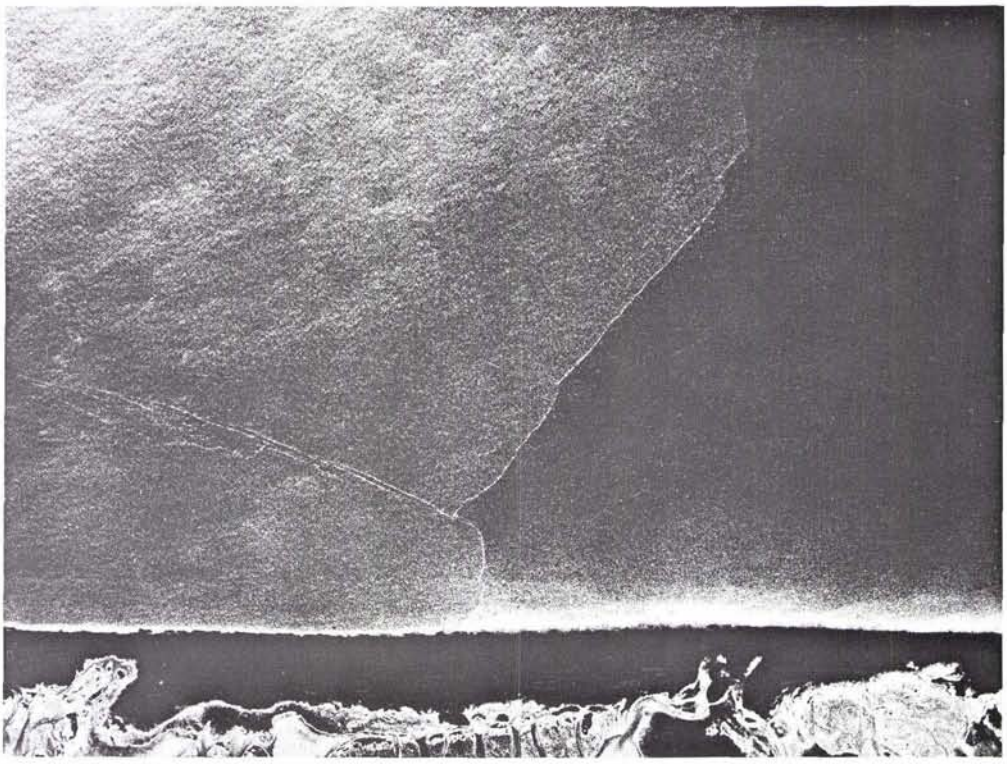

FIG. 4. High-contrast enhancement from the color photograph in Plate 1.

counts from water samples taken at the time of overflights averaged approximately 8 mg/liter over this entire area. A comparison of film density measurements with the suspended particulate counts over this area yielded no valid correlative information. Measurements made have demonstrated no correlation between the densities of the film and the total suspended material found in the water. More research is needed concerning the physics of back-scattered light from varying sizes, shapes, and types of particulate matter before valid comparisons can be established.

The plume front shown in Figure 4 was photographed three times during the day of November 17, 1970, spanning a total time of 146 minutes. The photographs were taken at 10:03, 10:26, and 12:29 EST. High-contrast enhancements were made from each of the three frames and a composite of the three enhancements was produced (Figure 5).

The composite of the three photographs illustrates the complex nature of the flow regime along a relatively uniform shoreline. A displacement analysis of the convergence zone or *front* (Figure 6) further illustrates the complexity of flow at four points, $P_1$ through $P_4$, along this front. These four points are recognizable features imaged in each of the three photographs and are used to plot displacement vectors during the 146-minute period. These vectors, although indicators of velocity, show only the composite displacement during the 146-minute period; however, they are the resultant of the velocity produced by the wind, and tidal currents existent during the time of the photographs.

A comparison of points $P_1$ and $P_2$ (Figure 6) illustrates the effects of flow resistance in the nearshore zone. The feature at $P_1$ lies just outside the breaker zone in very shallow water (5 m) whereas feature $P_2$ lies further offshore in a water depth of 15 m. The flow along the coast in the littoral zone should have a mean velocity considerably less than the waters offshore due to the higher resistance caused by the shallower depth and the rough surface of the bottom. This viscous drag will cause velocity to be lower near any solid boundary such as the bottom and the shoreline than it would be at a distance from these boundaries. In this example, with the two main velocity vectors (ebb current and

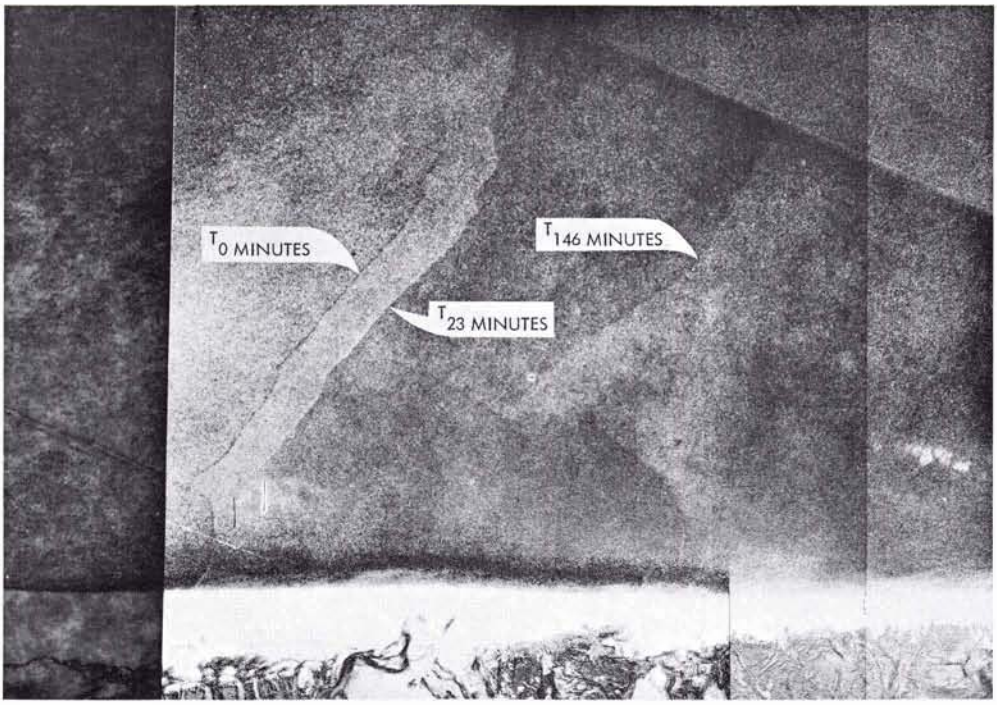


FIG. 5. Overlay of plume fronts photographed at 10:03, 10:26, and 12:29 EDT.

wind) both coming from a northeasterly direction, the effects of this flow resistance are clearly manifest in Figure 6 as less movement of the *front* in the littoral zone ($P_1$) in comparison with feature $P_2$ which is farther offshore.

The resultant displacement of feature $P_3$ can be attributed to the prevailing northeasterly wind-driven current and the offshore displacement by the estuarine discharge plume moving southerly along the coastline. The convergence line of this plume can be seen to be displaced farther offshore in each photograph, as well as moving southward. This offshore velocity component has caused the offshore displacement of both $P_3$ and $P_4$.

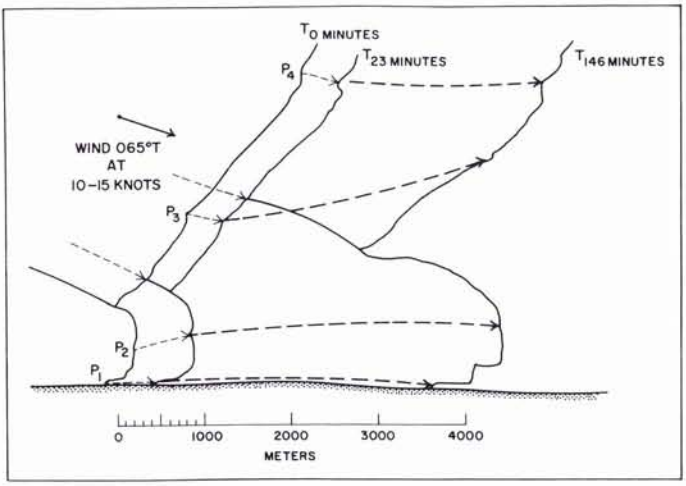


FIG. 6. The displacement of four points along a color front during an elasped time of 146 minutes.

However, the feature at $P_4$ has not been displaced by this offshore component to the extent that feature $P_3$ has, and is therefore influenced predominantly by the wind-driven current, and only secondarily by the discharge plume.

In May 1971 another technique for estuarine circulation studies was examined. In place of naturally occurring color fronts, dye implants were used to study the complex fluid flow dynamics in the Patuxent River estuary, Maryland. As in the November 1970 experiment, simultaneous surface truth measurements were taken during a series of low level overflights by the Naval Oceanographic Office's C-121 aircraft. The aircraft's objective was to collect repetitive color photographs and infrared imagery over the estuary while the ground team collected data from three water level stations, a surface thermistor

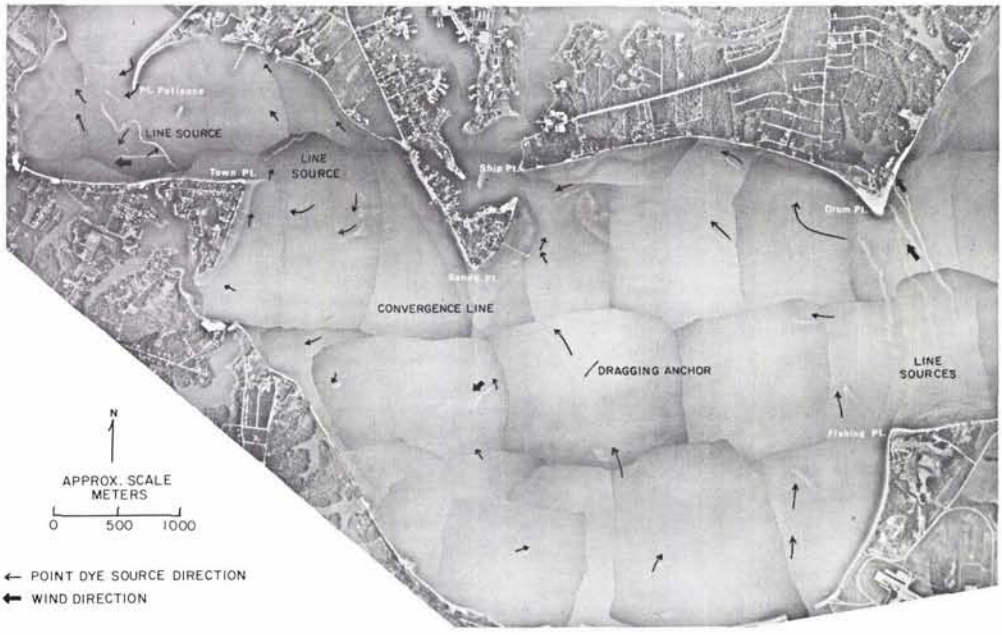


FIG. 7. Photographic mosaic of the Patuxent River estuary, 14 May 1971 (1642-1700 EDT).

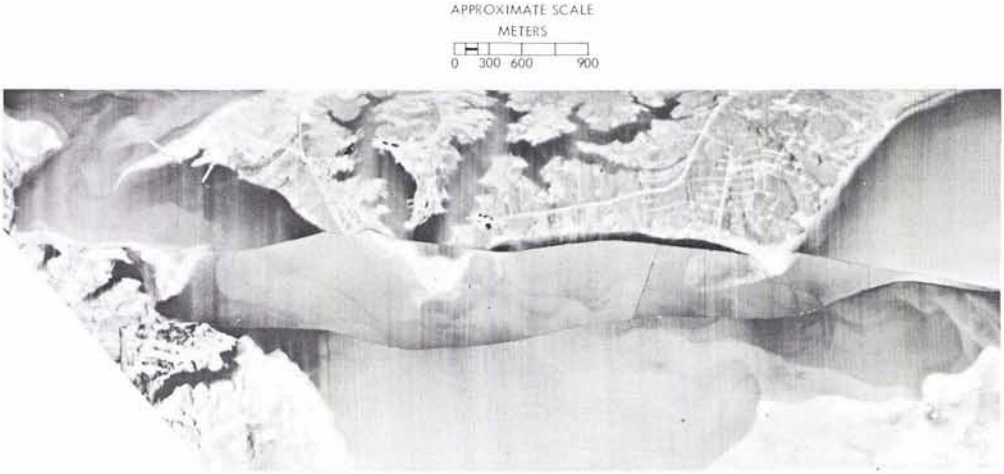


FIG. 8. Infrared mosaic of the Patuxent River estuary, 14 May 1971 (1642-1700 EDT).

chain, temperature and salinity transects, three moored current meters, wind direction, smoke bombs, point and continuous line dye sources, and subsurface light penetration equipment.

Mosaics constructed from the photographs (Figure 7) and the infrared imagery (Figure 8) illustrate the complex circulation within the estuary at the time of the overflight. Arrows were superimposed on the photographic mosaic to indicate the direction of the dye and smoke dispersal. The surface circulation within the estuary is uniquely depicted in the photo mosaic by the 35 point sources and the line sources located at three separate areas. One of the areas of particular interest is the eddy that exists during flood tide off Drum Point. The detail is difficult to distinguish in Figure 7 but in the original color photographs fluorescein dye from a point and a line source has been entrained into the eddy, enhancing its visibility. This eddy is also observed in the IR imagery (Figure 8) where the warmer water flows out from a shallow pond just north of Drum Point. This outflow provides a sharp thermal contrast as this water flows around Drum Point into the eddy.

Throughout the area the outflows of warmer water from the shallow creeks and coves provide sharp thermal discontinuities on the order of 1° to 2°C. The movements and positions of these thermal discontinuities in relation to the main stream flow provide information about flow direction, points of flow separation, eddy size, upwelling, and lines of water mass convergence. However, the utility of the IR imagery decreases as an ebb tidal phase is impressed on the area; the warmer waters are entrained and mixed into the main stream flow and the thermal contrast is greatly diminished.

Moving farther upstream, the complex flow structure that occurs as the tidal current progresses through successive bends of the river can be seen more clearly in Plate 2. Here the continuous line source, which was originally generated as a line between the tip of Point Patience and the opposite bank is rotating counter-clockwise as the main flow is channeled along the southeastern side of the Point. The point sources also illustrate a *choking* effect resulting in a partial flow reversal occurring along the lower bank. The *choking* effect is a result of insufficient *specific energy** to pass the increased discharge per unit width in this area of extreme channel contraction. (Henderson, 1966).

A qualitative streamline analysis (Figure 9) based on the composite photographic and IR imagery data serves to illustrate the benefit of such an approach for developing conceptual models. The boundaries of the rela-

* Specific energy is defined here as the energy referred to the channel bed as datum.

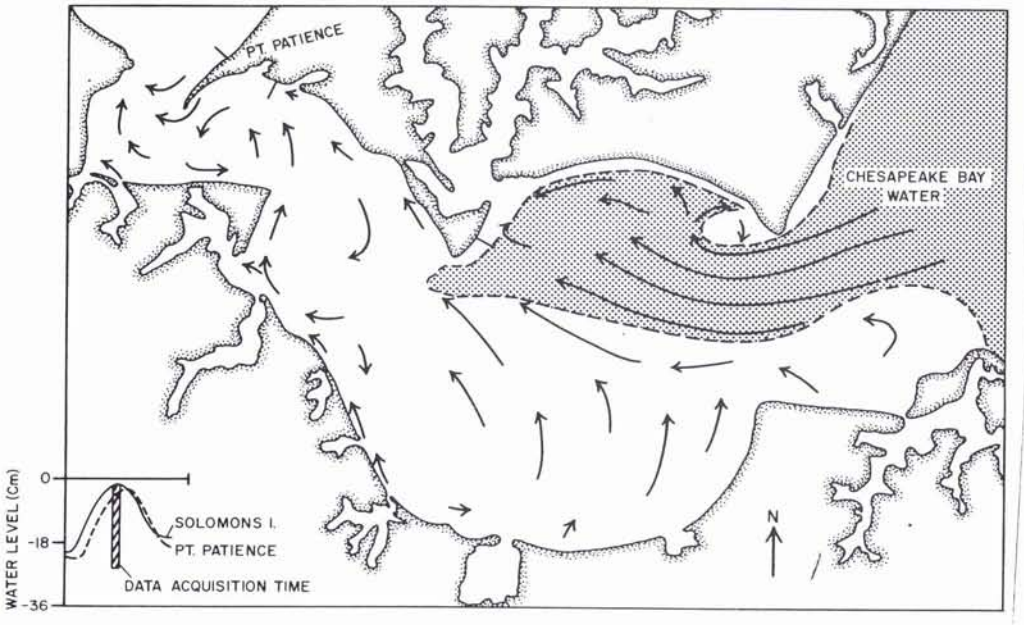


FIG. 9. Streamline analysis from composite dye tracer and IR imagery data.

tively unmixed Chesapeake Bay water were derived from positions of convergent line slicks in the photographs and thermal discontinuities in the IR imagery. Ground-truth surface temperature and salinity transects verified the upstream limit of this surface boundary. At this boundary the flow becomes increasingly unstable and less uniform as it passes into a contracting and bending channel. The Bay water is then mixed with and overridden by the warmer and less dense waters of the river but reappears upstream in areas of upwelling.

The two color photographs (Plates 3 and 4) taken 396 seconds apart at the mouth of the estuary during an ebb flow are used to illustrate a basic quantitative approach using short-term repetitive photographs of dye tracers. In the first photograph (Plate 3), a continuous line source is in the process of being generated between Fishing Point and Drum Point. Two point sources are dispersing dye adjacent to the line source. In addition, bayward of the new line source, the remnant of an older line source can be seen.

In the second photograph (Plate 4) the displacement of the line sources and the movement from the point sources during the 396-second time interval can be seen. The location of the dye images (with the exception of the new line source in Plate 4) were plotted (Figure 10) after the photographs were corrected for altitude and tilt differences. The center line of the line sources was then estimated and displacement measurements along with velocity calculations were made from these positions. The cross-sectional variations (Figure 10) of the surface velocities, $V_1$ through $V_8$, clearly indicate the high velocity area at the beginning of the abrupt channel contraction. The increased velocities of the point and remnant line sources, $V_9$ through $V_{10}$, are produced by the continuation of the narrowing channel and increased convergence.

Three current meters were taut-line moored 2.6 m below the surface between Drum Point and Fishing Point. One meter was moored in the vicinity of maximum displacement of the line sources (Figure 10). This displacement occurs to the right of the channel axis. The computed velocity, $V_3$, has a magnitude of 0.6 knot and the current recorded by the meter positioned as shown was indicating approximately the same direction at 0.5 knots.

This reasonable correlation was obtained from the water level and current speed data (Figure 11) taken during the photographic data-acquisition time and an extrapolated current-speed record. The extrapolation of earlier recorded current-speed data was necessitated by instrument failure prior to the overflight. The procedure for utilizing these

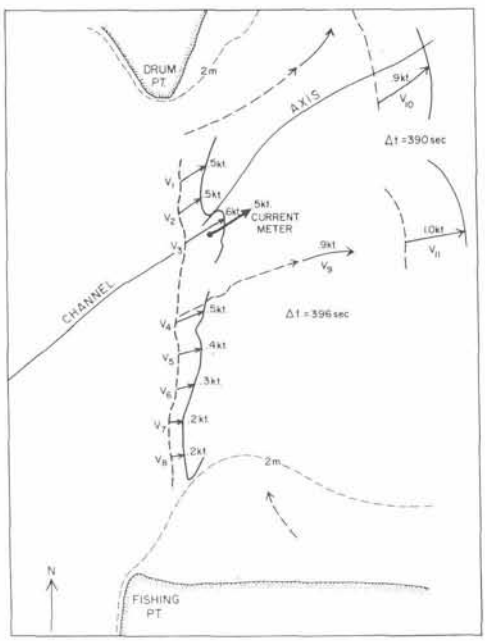


FIG. 10. Cross-sectional surface velocity calculations from line and point dye tracer sources.

data was to select a period in the water level data (when the current meter was functioning properly) that had approximately the same tidal phase and amplitude. As the amount of energy contributed by the tidal force is approximately the same and as no large variation in discharge occurred, the extrapolation should be reasonable. Completion of the processing of data from the other meters will provide a better correlation base.

## Summary and Conclusions

The objective of these investigations has been to develop a remote sensing methodology for the study of nearshore circulation dynamics using both natural and artificial color differences as circulation indicators. Both naturally occurring color fronts and dye implants have been used successfully in the interpretation of sequential multispectral aerial photographs and infrared imagery to deduce coastal and estuarine circulation dynamics. The results presented in this paper demonstrate that repetitive remotely sensed data coupled with a well equipped concurrent surface data collection program can provide extremely useful information on the complexity of estuarine flow.

It has also been shown that the temporal scale at which the coastal environment must be looked at to explain fully its dynamic nature is within the framework of minutes and hours. Therefore, it appears that studies of circulation dynamics in the nearshore area are properly within the realm of a well coordinated remote sensing program capable of repeat coverages on the temporal scale mentioned above.

## Acknowledgement

The authors wish to express their appreciation to the National Aeronautics and Space Administration, Manned Spacecraft Center, Houston, Texas, and the U.S. Naval Oceanographic Office, Suitland, Maryland for providing the remote sensing platforms necessary to conduct this research.

Grateful acknowledgement especially goes to John W. Sherman, III, NASA/Navy Spacecraft Oceanographic Project, whose support and recognition of our interests was responsible for the undertaking of these investigations.

A special thanks also goes to Kathleen LeFevre and Joseph Gattone for their innumerable services provided.

## References

Sherman, J. W., 1971, Remote Sensing Oceanography, *Proceedings of the International Workshop on Earth Resources Survey Systems*, University of Michigan, Vol. 1.

Yost, E., with Anderson, R., Kalia, R., Posteraro, V., and Wenderoth, S., 1971, Multispectral Photographic Remote Sensing of Coastal Environments, *Technical Report # 11, SERG TR-11*, Long Island University.

Henderson, F. M., 1966, *Open Channel Flow*, MacMillan Co., New York.

Polcyn, F. C. and Rollin, R. A., 1969, Remote Sensing Techniques for the Location and Measurement of Shallow Water Features, *Report # 8973-10-P*, Willow Run Laboratories. The University of Michigan, Ann Arbor.

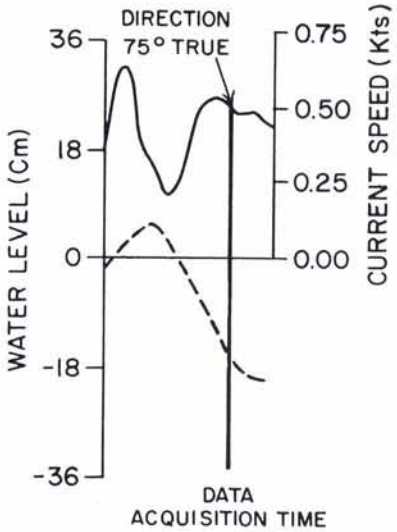


Fig. 11. Water level and current speed data.